Exclusive Study of $(g-2)_\mu$ HVP

Aaron S. Meyer (ameyer@quark.phy.bnl.gov)

Brookhaven National Laboratory

September 23, 2019

Lattice X Workshop 2019 - BNL

BROOKHAVEN NATIONAL LABORATORY

The RBC & UKQCD collaborations

BNL and BNL/RBRC

Yasumichi Aoki (KEK)
Taku Izubuchi
Yong-Chull Jang
Chulwoo Jung
Meifeng Lin
Aaron Meyer
Hiroshi Ohki
Shigemi Ohta (KEK)
Amarjit Soni

UC Boulder

Oliver Witzel

CERN

Mattia Bruno

Columbia University

Ryan Abbot
Norman Christ
Duo Guo
Christopher Kelly
Bob Mawhinney
Masaaki Tomii
Jiqun Tu
Bigeng Wang
Tianle Wang
Yidi Zhao

University of Connecticut

Tom Blum
Dan Hoying (BNL)
Luchang Jin (RBRC)
Cheng Tu

Edinburgh University

Peter Boyle
Luigi Del Debbio
Felix Erben
Vera Gülpers
Tadeusz Janowski
Julia Kettle
Michael Marshall
Fionn Ó hÓgáin
Antonin Portelli
Tobias Tsang
Andrew Yong
Azusa Yamaguchi

KEK

Julien Frison

University of Liverpool

Nicolas Garron

MIT

David Murphy

Peking University

Xu Feng

University of Regensburg

Christoph Lehner (BNL)

University of Southampton

Nils Asmussen
Jonathan Flynn
Ryan Hill
Andreas Jüttner
James Richings
Chris Sachrajda

Stony Brook University

Jun-Sik Yoo
Sergey Syritsyn (RBRC)

Outline

- Muon $g-2$ Experiment
  - Motivation from muon $g-2$
  - Tensions in $\pi\pi$ Scattering
  - Error Budget and LQCD Strategy
- Correlation Function Spectrum & Overlap
  - Lattice Parameters
  - GEVP Spectrum & Overlaps
  - $\pi\pi$ Scattering Phase Shift
  - 4π Correlation Functions
- Bounding Method and the Muon HVP
  - Correlation Function Reconstruction
  - (Improved) Bounding Method
  - Results
- Conclusions/Outlook

Introduction

Muon Anomalous Magnetic Moment Experiment

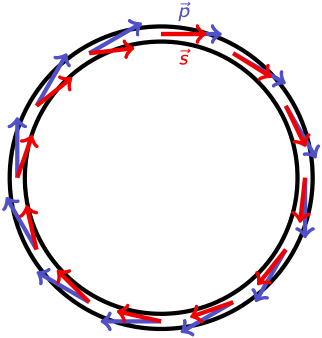

[Bennett *et al.*, 0602035[hep-ex]]

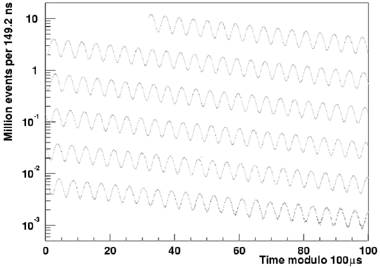

High-precision experiment of spin precession
relative to momentum direction in storage ring

Anomalous frequency $\omega_a = \frac{g-2}{2}\frac{eB}{m} = a_\mu \frac{eB}{m}$

Sensitive to new physics, and also discrepant with experiment!

Fermilab Muon $g-2$ Experiment



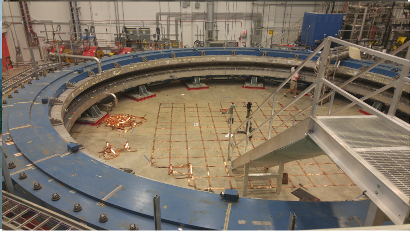

Experiment has come a long way (and so has theory!)

Aiming for a $4\times$ improvement in uncertainty over the BNL result

Muon $g-2$ Theory Error Budget

Contribution	Value $\times 10^{10}$	Uncertainty $\times 10^{10}$
QED	11 658 471.895	0.008
EW	15.4	0.1
HVP LO	692.5	2.7
HVP NLO	-9.84	0.06
HVP NNLO	1.24	0.01
Hadronic light-by-light	10.5	2.6
Total SM prediction	11 659 181.7	3.8
BNL E821 result	11 659 209.1	6.3
Fermilab E989 target		≈ 1.6

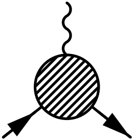

Experiment-Theory difference is 27.4(7.3) $\implies$ 3.7σ tension!

Target measurement: Hadronic Vacuum Polarization (HVP)

$\implies$ Lattice results have larger uncertainty, but systematically improve

$\implies$ Dispersive ("R-ratio") results more precise, but static

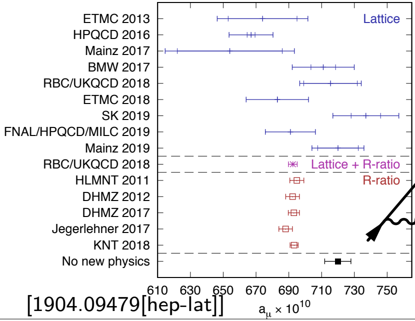

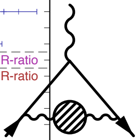

[1904.09479[hep-lat]]

Tensions in Experiment

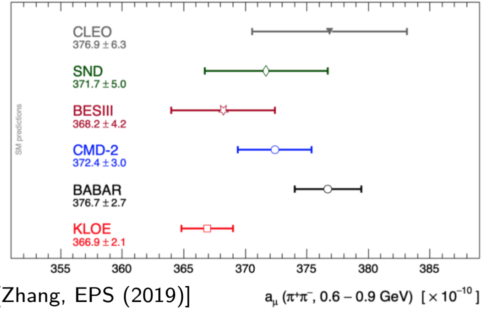

[Zhang, EPS (2019)]

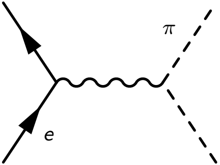

R-ratio data for $ee \to \pi\pi$ exclusive channel, $\sqrt{s} = 0.6 - 0.9\ \mathrm{GeV}$ region
Tension between most precise measurements (BABAR/KLOE)
R-ratio a_μ^{HVP} uncertainty $<$ difference in this channel

Avoid tension by computing precise lattice-only estimate of a_μ^{HVP}
Use lattice QCD to inform experiment, resolve discrepancy

Exclusive Channels in the HVP

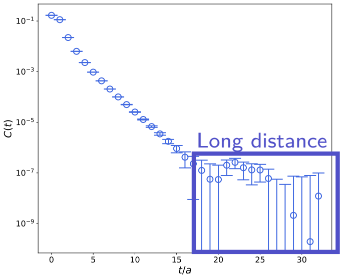

$$C(t) = \frac{1}{3}\sum_i \left\langle \left[\bar{\psi}\gamma_i\psi\right]_t \left[\bar{\psi}\gamma_i\psi\right]_0 \right\rangle$$

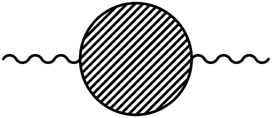

Correlator has large statistical error in long-distance region,
but contributions from high energy states are exponentially suppressed

Long distance correlator dominated by two-pion states,
but overlap of vector current with two-pion states is minimal

Exclusive Channels in the HVP

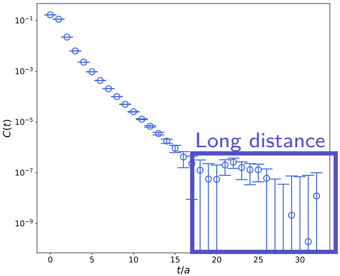

$$C(t) = \frac{1}{3}\sum_i \left\langle \left[\bar{\psi}\gamma_i\psi\right]_t \left[\bar{\psi}\gamma_i\psi\right]_0 \right\rangle$$
$$\approx \sum_n \left| \langle \Omega|\bar{\psi}\gamma_i\psi|n\rangle \right|^2 e^{-E_n t}$$

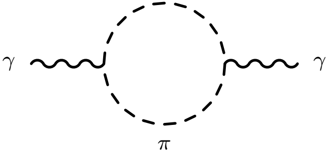

Correlator has large statistical error in long-distance region,
but contributions from high energy states are exponentially suppressed

Long distance correlator dominated by two-pion states,
but overlap of vector current with two-pion states is minimal

Strategy:

- Construct & measure operators that overlap strongly with $\pi\pi$ states
- Correlate these operators with the local vector current
- a_μ^{HVP} computed by integrating with time-momentum representation kernel,
  $a_\mu^{HVP} = \sum_t w_t C(t)$ [D.Bernecker & H.Meyer, 1107.4388 [hep-lat]]

Computation Setup

Ensemble Details

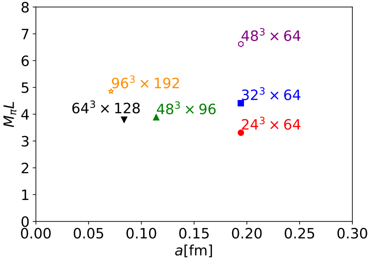

Computed on $2+1$ flavor Möbius Domain Wall Fermions for valance and sea, M_π at physical value on all ensembles

Computations using distillation setup

24^3 and 32^3 ($+48^3$) ensembles $\rightarrow$ infinite volume limit
48^3 and 64^3 ($+96^3$) ensembles $\rightarrow$ continuum limit

Compare results of explicit calculation of finite volume results to Luscher + Gounaris-Sakurai prediction [H.Meyer, 1107.4388[hep-lat]]

Not presented here, see [C.Lehner, Lattice 2018]

Operators

Operators constructed in $I = 1$, P-wave channel to impact upon HVP_μ

Designed to have strong overlap with specific target states,
but all operators unavoidably couple to all states in HVP spectrum

Vector current operators:

- Local $\mathcal{O}_{J_\mu} = \sum_x \bar{\psi}(x)\gamma_\mu\psi(x)$, $\mu \in \{1,2,3\}$
- Smeared $\mathcal{O}_{j_\mu} = \sum_{xyz} \bar{\psi}(x) f(x-z)\gamma_\mu f(z-y)\psi(y)$

2π operators with $\mathcal{O}_n$ given by $\vec{p}_\pi \in \frac{2\pi}{L} \times \{(1,0,0),(1,1,0),(1,1,1),(2,0,0)\}$

$$\mathcal{O}_n = \left| \sum_{xyz} \bar{\psi}(x) f(x-z) e^{-i\vec{p}_\pi\cdot\vec{z}} \gamma_5 f(z-y)\psi(y) \right|^2$$

Also test two 4π operators with $\vec{p}_\pi = \frac{2\pi}{L} \times (1,0,0)$:

$$\mathcal{O}_{4\pi} = \left| \sum_{xyz} \bar{\psi}(x) f(x-z) e^{-i\vec{p}_\pi\cdot\vec{z}} \gamma_5 f(z-y)\psi(y) \right|^2 \left| \sum_{xy} \bar{\psi}(x) f(x-y)\gamma_5\psi(y) \right|^2$$

Correlators arranged in a $N \times N$ symmetric matrix:

$\otimes$	$\mathcal{O}_{J_\mu}$	$\mathcal{O}_{j_\mu}$	$\mathcal{O}_{2\pi}$	$\mathcal{O}_{4\pi}$
$\mathcal{O}_{J_\mu}$	$C_{J_\mu J_\mu}$	$C_{J_\mu j_\mu}$	$C_{J_\mu 2\pi}$	$C_{J_\mu 4\pi}$
$\mathcal{O}_{j_\mu}$		$C_{j_\mu j_\mu}$	$C_{j_\mu 2\pi}$	$C_{j_\mu 4\pi}$
$\mathcal{O}_{2\pi}$			$C_{2\pi 2\pi}$	$C_{2\pi 4\pi}$
$\mathcal{O}_{4\pi}$				$C_{4\pi 4\pi}$

$\rightarrow C(t)$

Generalized EigenValue Problem (GEVP)

Generalized EigenValue Problem to estimate overlap with vector current & energies

$$C(t)\, V = C(t + \delta t)\, V\, \Lambda(\delta t)$$

$$\Lambda_{nn}(\delta t) \sim e^{+E_n \delta t}\,, \quad V_{im} \propto \langle\Omega|\, \mathcal{O}_i\, |m\rangle$$

$C(t)$ is the matrix of correlation functions from previous slide

Compute at fixed δt, vary t: plateau for large t

From result, reconstruct exponential dependence of local vector correlation function

$$C_{ij}^{\text{latt.}}(t) = \sum_{n}^{N} \langle\Omega|\, \mathcal{O}_i\, |n\rangle\, \langle n|\, \mathcal{O}_j\, |\Omega\rangle\, e^{-E_n t}$$

In theory, infinite number of states contribute to correlation function

In practice, only finite N necessary to model correlation function

$\implies$ finite GEVP basis is sufficient

GEVP Results - $J_\mu + 2\pi$ Operators only

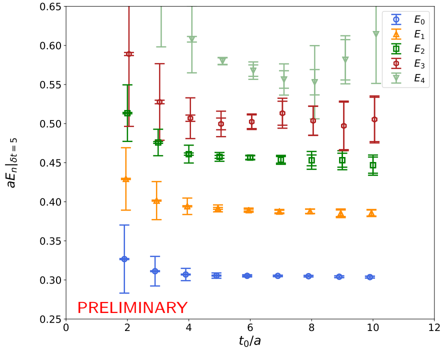

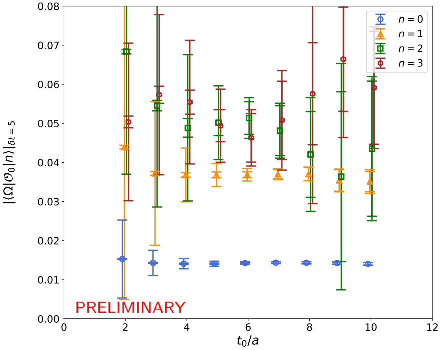

6-operator basis on 48I ensemble: local+smeared vector, $4\times(2\pi)$

Data points from solving GEVP at fixed δt

$$C(t_0)\,V = C(t_0+\delta t)\,V\,\Lambda(\delta t)\,, \quad \Lambda_{nn}(\delta t) \sim e^{+E_n\delta t}$$

Excited state contaminations decay as $t_0, \delta t \to \infty$
moving right on plot $\implies$ asymptote to lowest states' spectrum & overlaps

Statistics+systematics; Left: Spectrum; Right: Overlap with local vector current

Phase Shift

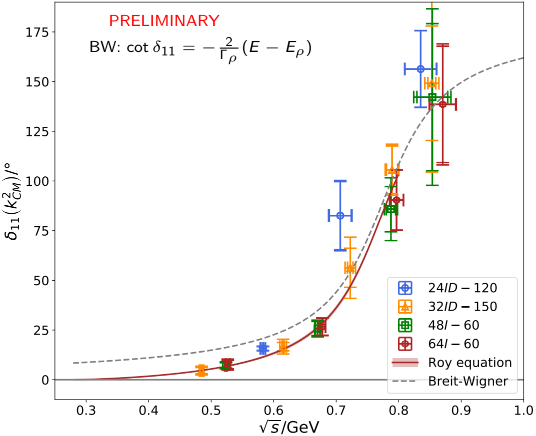

Compute $\pi\pi$ scattering phase shifts in $I = 1$ channel from spectrum
Statistics + systematics

Compare to simple Breit-Wigner parametrization and pheno (courtesy of M.Bruno)
Good agreement with pheno for 32ID, 48I, 64I
24ID: remnant excited state contaminations, still to be removed

Scattering phase shift results to appear as part of series of papers by RBC+UKQCD

Phase Shift

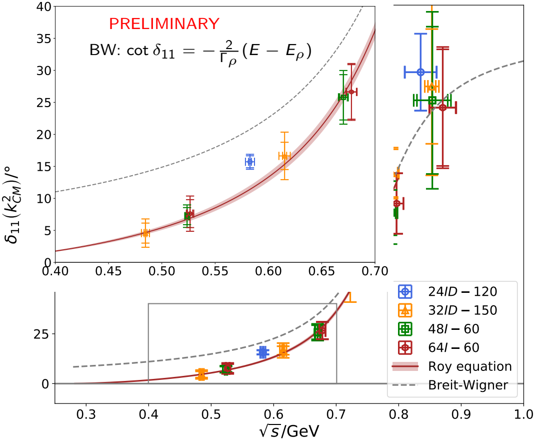

Compute $\pi\pi$ scattering phase shifts in $I = 1$ channel from spectrum
Statistics + systematics

Compare to simple Breit-Wigner parametrization and pheno (courtesy of M.Bruno)
Good agreement with pheno for 32ID, 48I, 64I
24ID: remnant excited state contaminations, still to be removed

Scattering phase shift results to appear as part of series of papers by RBC+UKQCD

Group Theory & Contraction Engine

An automated group theory engine has been an integral part of RBC-UKQCD's automated setup for two-pion diagrams in exclusive channel study

Group Theory & Contraction Engine

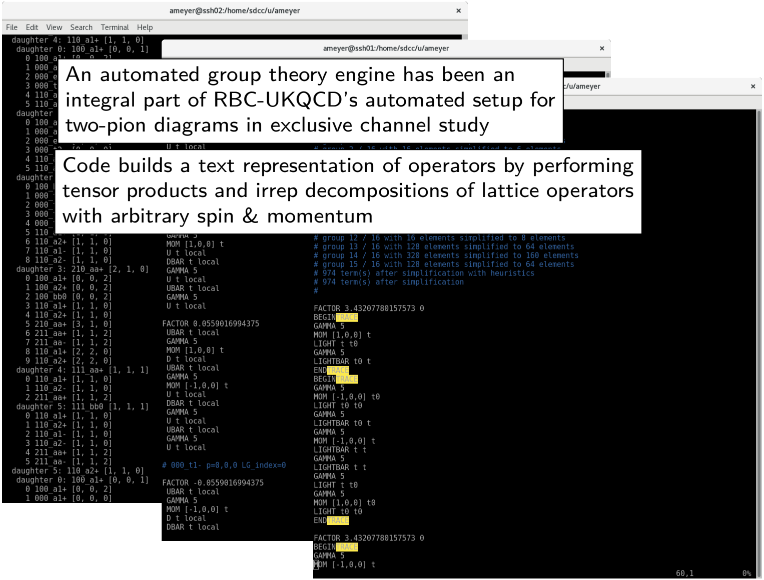

An automated group theory engine has been an integral part of RBC-UKQCD's automated setup for two-pion diagrams in exclusive channel study

Code builds a text representation of operators by performing tensor products and irrep decompositions of lattice operators with arbitrary spin & momentum

Group Theory & Contraction Engine

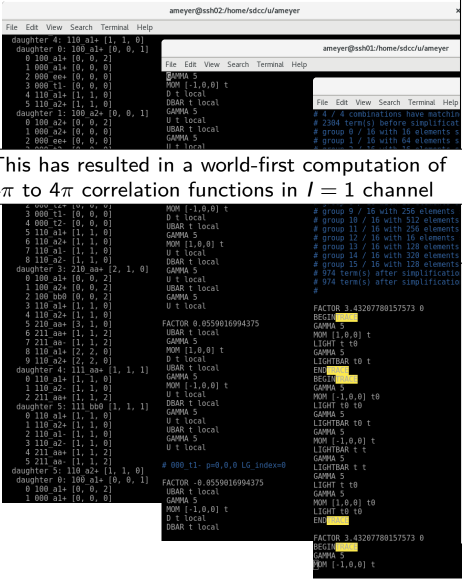

This has resulted in a world-first computation of 4π to 4π correlation functions in $I = 1$ channel

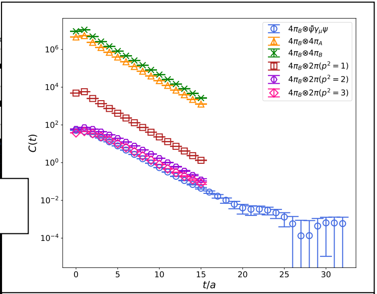

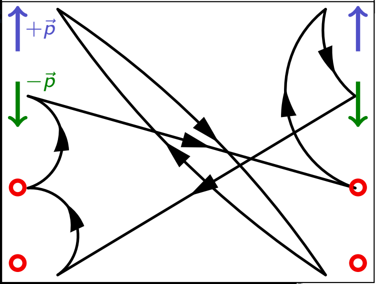

4π Contractions

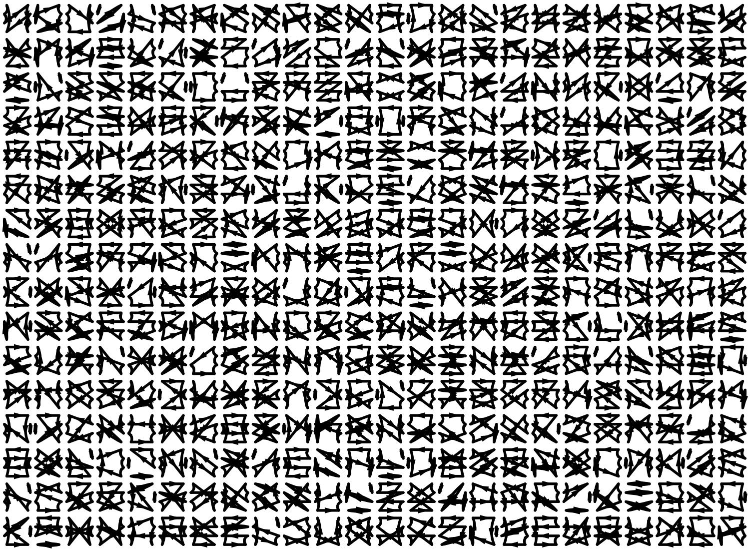

4π Contractions cont...

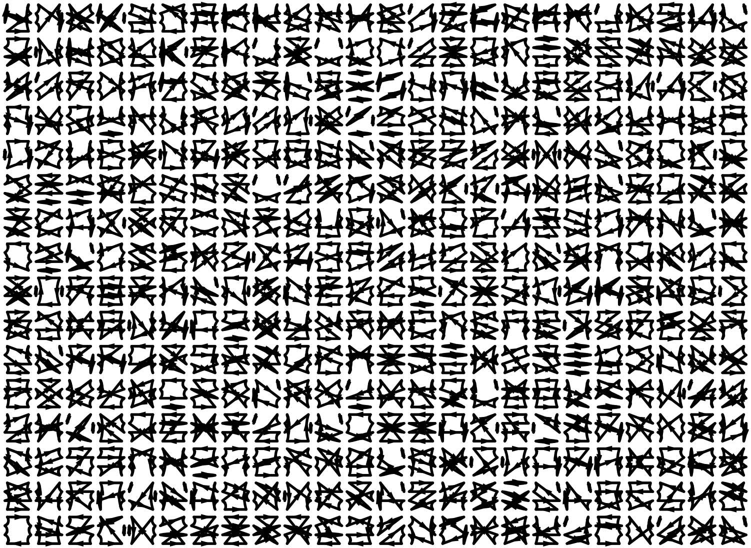

4π Contractions cont... cont...

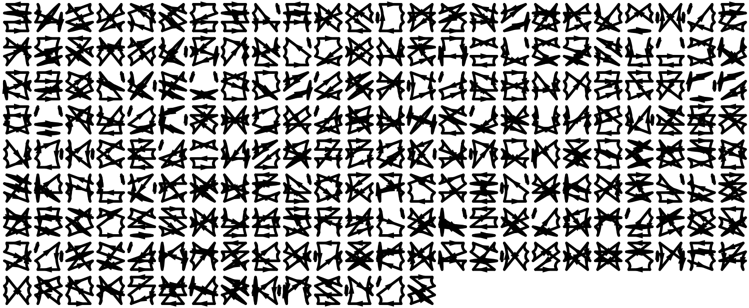

GEVP Results - 4π Operators

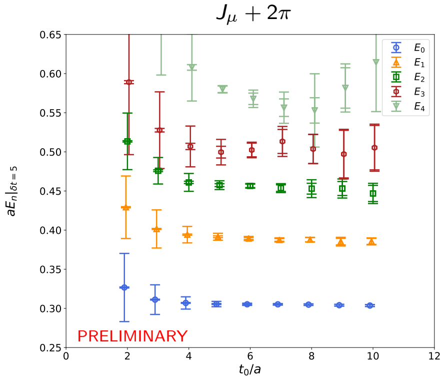

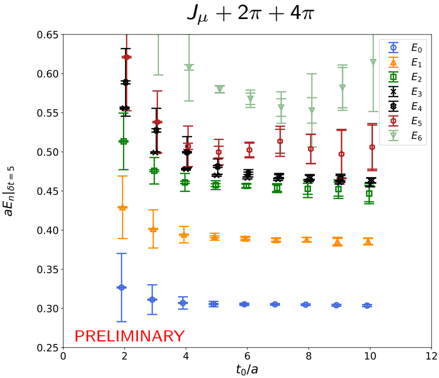

Extra 4π states could appear with overlap to local vector current
Breakdown of formalism for FVC could occur at 4π threshold

Results unaffected by inclusion of 4π operators, but states resolvable

GEVP Results - 4π Operators

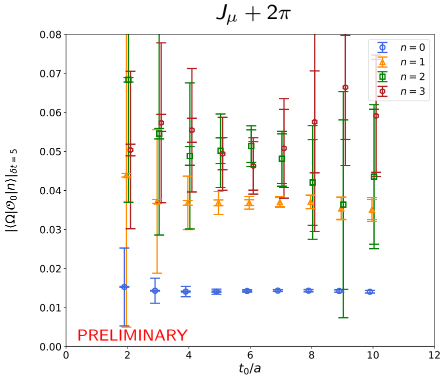

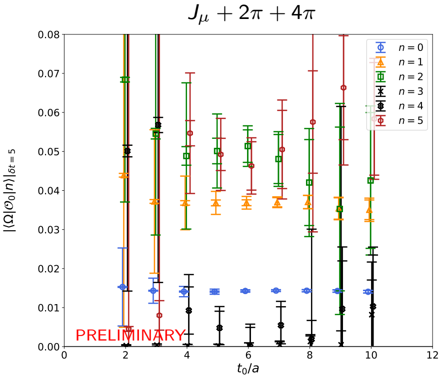

Extra 4π states could appear with overlap to local vector current
Breakdown of formalism for FVC could occur at 4π threshold

Results unaffected by inclusion of 4π operators, but states resolvable

Overlap of 4π states with local vector current unresolvable

GEVP Results - 4π Operators

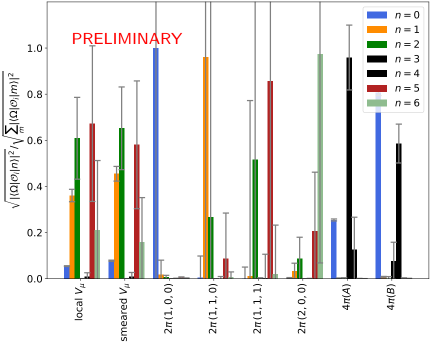

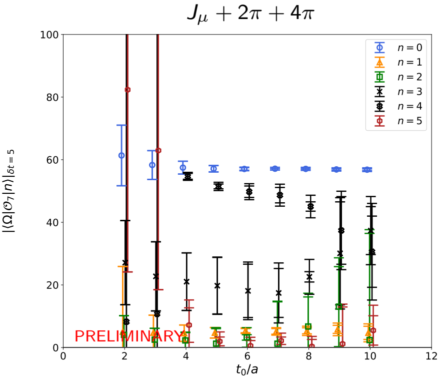

Extra 4π states could appear with overlap to local vector current
Breakdown of formalism for FVC could occur at 4π threshold

Results unaffected by inclusion of 4π operators, but states resolvable

Overlap of 4π states with local vector current unresolvable

Overlap of states with 4π operator significant
$\implies$ 4π state safely negligible in local vector current
$\implies$ Will be neglected in all of following analysis

Correlator Reconstruction and Bounding

Correlation Function Reconstruction - 48I

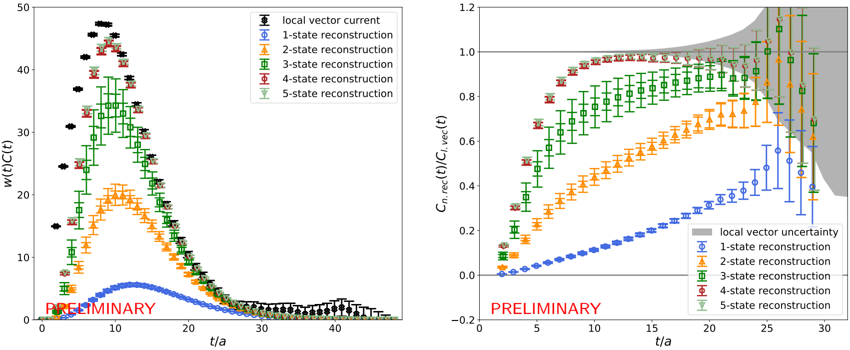

Plotted: (weight kernel) $\times$ (correlation function); integral $\rightarrow a_{\mu}^{HVP}$

GEVP results to reconstruct long-distance behavior of
local vector correlation function needed to compute connected HVP

Explicit reconstruction good estimate of correlation function at long-distance,
missing excited states at short-distance

More states $\implies$ better reconstruction, can replace $C(t)$ at shorter distances

Improved Bounding Method

Use known results in spectrum to make a precise estimate of upper & lower bound on a_μ^{HVP} [RBC (2017)]

$$\widetilde{C}(t; t_{\max}, E) = \begin{cases} C(t) & t < t_{\max} \\ C(t_{\max}) e^{-E(t-t_{\max})} & t \geq t_{\max} \end{cases}$$

Upper bound: $E \leq E_0$, lowest state in spectrum

Lower bound: $E \geq \log[\frac{C(t_{\max})}{C(t_{\max}+1)}]$

BMW Collaboration [K.Miura, Lattice2018] takes $E \to \infty$

With good control over lower states in spectrum from exclusive reconstruction, improve bounding method [RBC/UKQCD 2018 (CL@KEK Feb 2018)]:

Replace $C(t) \to C(t) - \sum_n^N |c_n|^2 e^{-E_n t}$ and apply bounding procedure for $a_\mu - \delta a_\mu$

$\implies$ Long distance convergence now $\propto e^{-E_{N+1} t}$, lower bound falls faster

$\implies$ Smaller overall contribution from neglected states

After bounding, add back $\delta a_\mu = \sum_{t=t_{\max}}^{\infty} w_t \sum_n^N |c_n|^2 e^{-E_n t}$

Bounding Method Results - 48I

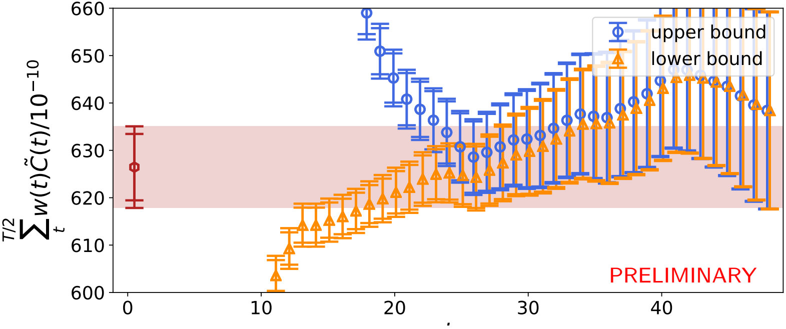

No bounding method: $a_\mu^{HVP} = 638(21)$

Bounding method $t_{\max} = 3.3\ \mathrm{fm}$, no reconstruction: $a_\mu^{HVP} = 626.5(8.6)$

Bounding method gives factor of 3 improvement over no bounding method

Bounding Method Results - 48I

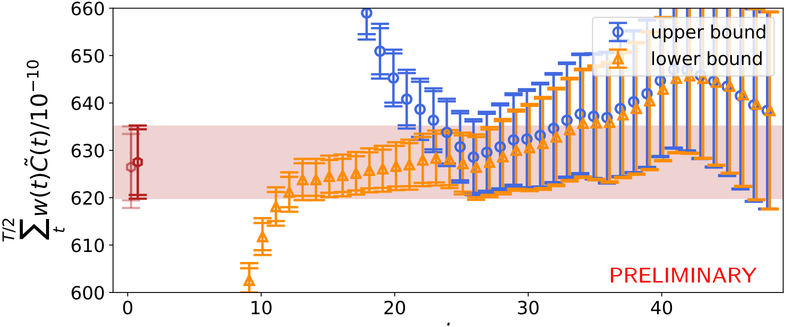

No bounding method:	$a_\mu^{HVP} = 638(21)$
Bounding method $t_{\text{max}} = 3.3$ fm, no reconstruction:	$a_\mu^{HVP} = 626.5(8.6)$
Bounding method $t_{\text{max}} = 3.0$ fm, 1 state reconstruction:	$a_\mu^{HVP} = 627.5(7.7)$

Bounding method gives factor of 3 improvement over no bounding method

Bounding Method Results - 48I

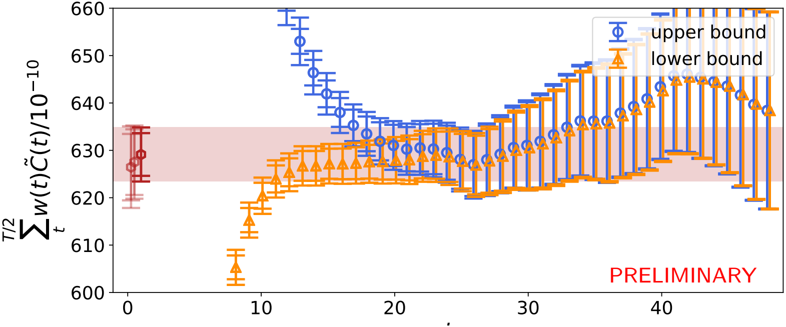

No bounding method:	$a_\mu^{HVP} = 638(21)$
Bounding method $t_{\max} = 3.3\ \mathrm{fm}$, no reconstruction:	$a_\mu^{HVP} = 626.5(8.6)$
Bounding method $t_{\max} = 3.0\ \mathrm{fm}$, 1 state reconstruction:	$a_\mu^{HVP} = 627.5(7.7)$
Bounding method $t_{\max} = 2.9\ \mathrm{fm}$, 2 state reconstruction:	$a_\mu^{HVP} = 629.1(5.7)$

Bounding method gives factor of 3 improvement over no bounding method

Bounding Method Results - 48I

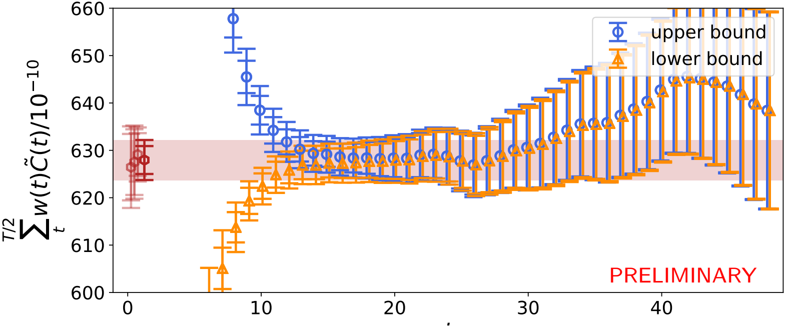

No bounding method: $a_\mu^{HVP} = 638(21)$

Bounding method $t_{\max} = 3.3$ fm, no reconstruction: $a_\mu^{HVP} = 626.5(8.6)$

Bounding method $t_{\max} = 3.0$ fm, 1 state reconstruction: $a_\mu^{HVP} = 627.5(7.7)$

Bounding method $t_{\max} = 2.9$ fm, 2 state reconstruction: $a_\mu^{HVP} = 629.1(5.7)$

Bounding method $t_{\max} = 2.2$ fm, 3 state reconstruction: $a_\mu^{HVP} = 628.0(4.2)$

Bounding method gives factor of 3 improvement over no bounding method

Bounding Method Results - 48I

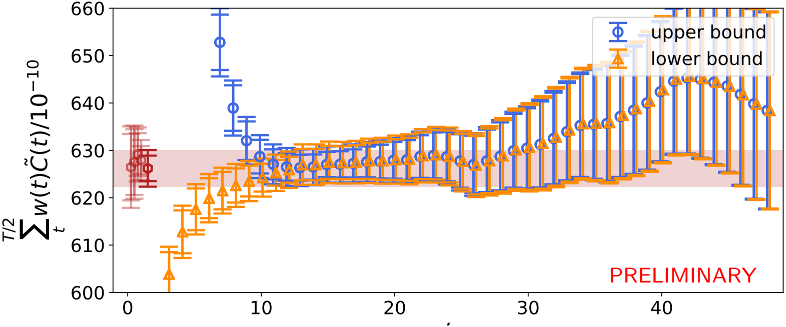

No bounding method: $a_\mu^{HVP} = 638(21)$

Bounding method $t_{\text{max}} = 3.3$ fm, no reconstruction: $a_\mu^{HVP} = 626.5(8.6)$

Bounding method $t_{\text{max}} = 3.0$ fm, 1 state reconstruction: $a_\mu^{HVP} = 627.5(7.7)$

Bounding method $t_{\text{max}} = 2.9$ fm, 2 state reconstruction: $a_\mu^{HVP} = 629.1(5.7)$

Bounding method $t_{\text{max}} = 2.2$ fm, 3 state reconstruction: $a_\mu^{HVP} = 628.0(4.2)$

Bounding method $t_{\text{max}} = 1.8$ fm, 4 state reconstruction: $a_\mu^{HVP} = 626.2(3.9)$

Bounding method gives factor of 3 improvement over no bounding method
Improving the bounding method increases gain to factor of 5, including systematics
Improvement should make all-lattice computation of a_μ^{HVP} competitive with R-ratio by 2020

Error Budget and Timeline

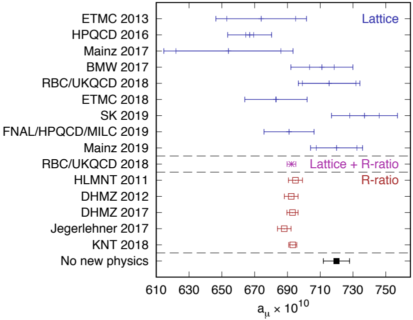

Update to RBC-UKQCD calculation including exclusive study in preparation

$\implies$ on target for precision improvement on a_μ^{HVP} at 5×10^{-10} level

Further reduction will require full RBC-UKQCD program of computations

Work on the exclusive channel study using bounding method has led to world-first estimation of finite volume corrections to a_μ^{HVP} at physical M_π

Complete analysis with full suite of systematic improvements ongoing
$\implies$ precision improvement $\times 10$ over original, target error on a_μ^{HVP} at 1×10^{-10}

Compare to dispersive $(3-5) \times 10^{-10}$

Conclusions

Conclusions

Pion scattering exlusive study poised to improve theory preicision in $(g-2)_\mu$:

- Dispersive approaches have unresolved tension in $\pi\pi$ scattering region, circumvented by LQCD calculation
- Computed $2\pi \to 4\pi$, $4\pi \to 4\pi$ correlation functions to show explicitly that 4π state has negligible effect on HVP at physical M_π
- Study of exclusive channels able to significantly reduce statistical uncertainty on an all-lattice computation of a_μ^{HVP}
  $\Longrightarrow$ expect to reach precision of $O(5 \times 10^{-10})$ by the end of year
  $\Longrightarrow$ target $O(1 \times 10^{-10})$ for all-lattice calculation
- Part of ongoing lattice study to address all lattice systematics in RBC+UKQCD HVP computation (see [C.Lehner, Lattice 2019])
- New data on 64^3 ensemble being analyzed
- Paper in progress; posting planned before end of year

Thank you!

BACKUP

Error Budget

$a_\mu^{\text{ud, conn, isospin}}$	$202.9(1.4)_{\rm S}(0.2)_{\rm C}(0.1)_{\rm V}(0.2)_{\rm A}(0.2)_{\rm Z}$	$649.7(14.2)_{\rm S}(2.8)_{\rm C}(3.7)_{\rm V}(1.5)_{\rm A}(0.4)_{\rm Z}(0.1)_{\rm E48}(0.1)_{\rm E64}$
$a_\mu^{\text{s, conn, isospin}}$	$27.0(0.2)_{\rm S}(0.0)_{\rm C}(0.1)_{\rm A}(0.0)_{\rm Z}$	$53.2(0.4)_{\rm S}(0.0)_{\rm C}(0.3)_{\rm A}(0.0)_{\rm Z}$
$a_\mu^{\text{c, conn, isospin}}$	$3.0(0.0)_{\rm S}(0.1)_{\rm C}(0.0)_{\rm Z}(0.0)_{\rm M}$	$14.3(0.0)_{\rm S}(0.7)_{\rm C}(0.1)_{\rm Z}(0.0)_{\rm M}$
$a_\mu^{\text{uds, disc, isospin}}$	$-1.0(0.1)_{\rm S}(0.0)_{\rm C}(0.0)_{\rm V}(0.0)_{\rm A}(0.0)_{\rm Z}$	$-11.2(3.3)_{\rm S}(0.4)_{\rm V}(2.3)_{\rm L}$
$a_\mu^{\text{QED, conn}}$	$0.2(0.2)_{\rm S}(0.0)_{\rm C}(0.0)_{\rm V}(0.0)_{\rm A}(0.0)_{\rm Z}(0.0)_{\rm E}$	$5.9(5.7)_{\rm S}(0.3)_{\rm C}(1.2)_{\rm V}(0.0)_{\rm A}(0.0)_{\rm Z}(1.1)_{\rm E}$
$a_\mu^{\text{QED, disc}}$	$-0.2(0.1)_{\rm S}(0.0)_{\rm C}(0.0)_{\rm V}(0.0)_{\rm A}(0.0)_{\rm Z}(0.0)_{\rm E}$	$-6.9(2.1)_{\rm S}(0.4)_{\rm C}(1.4)_{\rm V}(0.0)_{\rm A}(0.0)_{\rm Z}(1.3)_{\rm E}$
a_μ^{SIB}	$0.1(0.2)_{\rm S}(0.0)_{\rm C}(0.2)_{\rm V}(0.0)_{\rm A}(0.0)_{\rm Z}(0.0)_{\rm E48}$	$10.6(4.3)_{\rm S}(0.6)_{\rm C}(6.6)_{\rm V}(0.1)_{\rm A}(0.0)_{\rm Z}(1.3)_{\rm E48}$
$a_\mu^{\text{udsc, isospin}}$	$231.9(1.4)_{\rm S}(0.2)_{\rm C}(0.1)_{\rm V}(0.3)_{\rm A}(0.2)_{\rm Z}(0.0)_{\rm M}$	$705.9(14.6)_{\rm S}(2.9)_{\rm C}(3.7)_{\rm V}(1.8)_{\rm A}(0.4)_{\rm Z}(2.3)_{\rm L}(0.1)_{\rm E48}$ $(0.1)_{\rm E64}(0.0)_{\rm M}$
$a_\mu^{\text{QED, SIB}}$	$0.1(0.3)_{\rm S}(0.0)_{\rm C}(0.2)_{\rm V}(0.0)_{\rm A}(0.0)_{\rm Z}(0.0)_{\rm E}(0.0)_{\rm E48}$	$9.5(7.4)_{\rm S}(0.7)_{\rm C}(6.9)_{\rm V}(0.1)_{\rm A}(0.0)_{\rm Z}(1.7)_{\rm E}(1.3)_{\rm E48}$
$a_\mu^{\text{R-ratio}}$	$460.4(0.7)_{\rm RST}(2.1)_{\rm RSY}$	
a_μ	$692.5(1.4)_{\rm S}(0.2)_{\rm C}(0.2)_{\rm V}(0.3)_{\rm A}(0.2)_{\rm Z}(0.0)_{\rm E}(0.0)_{\rm E48}$ $(0.0)_{\rm b}(0.1)_{\rm c}(0.0)_{\overline{\rm S}}(0.0)_{\overline{\rm Q}}(0.0)_{\rm M}(0.7)_{\rm RST}(2.1)_{\rm RSY}$	$715.4(16.3)_{\rm S}(3.0)_{\rm C}(7.8)_{\rm V}(1.9)_{\rm A}(0.4)_{\rm Z}(1.7)_{\rm E}(2.3)_{\rm L}$ $(1.5)_{\rm E48}(0.1)_{\rm E64}(0.3)_{\rm b}(0.2)_{\rm c}(1.1)_{\overline{\rm S}}(0.3)_{\overline{\rm Q}}(0.0)_{\rm M}$

TABLE I. Individual and summed contributions to a_μ multiplied by 10^{10}. The left column lists results for the window method with $t_0 = 0.4$ fm and $t_1 = 1$ fm. The right column shows results for the pure first-principles lattice calculation. The respective uncertainties are defined in the main text.

[Blum *et al.*, (2018)]

Full program of computations to reduce uncertainties:

Reduce statistical uncertainties on light connected contribution

Compute QED contribution

Improve lattice spacing determination

Finite volume and continuum extrapolation study

First constrain the p-wave phase shift from our $L = 6.22$ fm physical pion mass lattice:

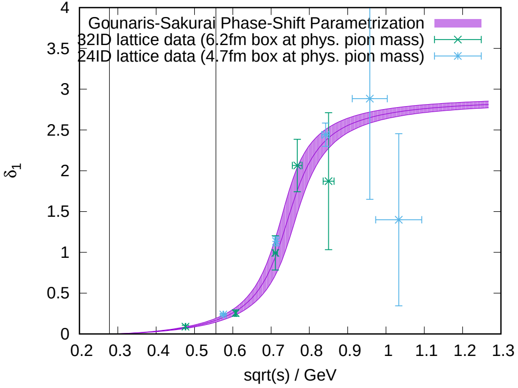

$E_\rho = 0.766(21)$ GeV (PDG 0.77549(34) GeV)
$\Gamma_\rho = 0.139(18)$ GeV (PDG 0.1462(7) GeV)

[Lehner, Mainz 2018]

Predicts $|F_\pi(s)|^2$:

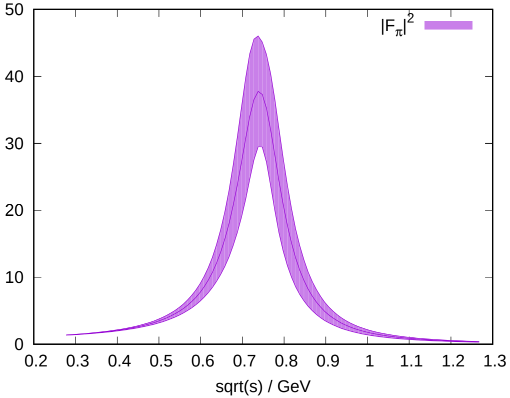

We can then also predict matrix elements and energies for our other lattices; successfully checked!

[Lehner, Mainz 2018]

Finite Volume Corrections on the Lattice

Complete error budget needs extrapolation to infinite volume

FV shift can be measured directly from results of exclusive study
$\Longrightarrow$ First time this shift resolved from zero at physical M_π!
$\Longrightarrow$ Previous bound at $10(26) \times 10^{-10}$, $M_\pi = 146\ \mathrm{MeV}$ [1805.04250[hep-lat]]

Can compare FV shift predictions from phenomenological estimations:
Gounaris-Sakurai-Lüscher, proposed by H.Meyer
[Phys.Rev.Lett. 21, 244; Nucl.Phys.B 354; Phys.Rev.Lett. 107, 072002]
and scalar QED

$$a_\mu^{HVP}(L = 6.2\ \mathrm{fm}) - a_\mu^{HVP}(L = 4.7\ \mathrm{fm}) = \begin{cases} 21.6(6.3) \times 10^{-10} & \text{LQCD} \\ 20(3) \times 10^{-10} & \text{GSL} \\ 12.2 \times 10^{-10} & \text{sQED} \end{cases}$$

Good agreement with GSL in range of energies probed by LQCD